JOURNAL OF GEOPHYSICAL RESEARCH, VOL. 104, NO. D16, PAGES 19,691–19,703, AUGUST 27, 1999

An evaluation of NEXRAD precipitation estimates in complex terrain

C. Bryan Young, [1] Brian R. Nelson, [1] A. Allen Bradley, [1] James A. Smith, [2] Christa D. Peters-Lidard, [3] Anton Kruger, [1] and Mary Lynn Baeck[2]

Abstract. Next Generation Weather Radar (NEXRAD) precipitation estimates are used for hydrological, meteorological, and climatological studies at a wide range of spatial and temporal scales. The utility of radar-based precipitation estimates in such applications hinges on an understanding of the sources and magnitude of estimation error. This study examines precipitation estimation in the complex mountainous terrain of the northern Appalachian Mountains. Hourly digital precipitation (HDP) products for two WSR-88D radars in New York state are evaluated for a 2-year period. This analysis includes evaluation of range dependence and spatial distribution of estimates, radar intercomparisons for the overlap region, and radar-gage comparisons. The results indicate that there are unique challenges for radar-rainfall estimation in mountainous terrain. Beam blockage is a serious problem that is not corrected by existing NEXRAD algorithms. Underestimation and nondetection of precipitation are also significant concerns. Improved algorithms are needed for merging estimates from multiple radars with spatially variable biases.

1. Introduction

The Next Generation Weather Radar (NEXRAD) network of WSR-88D (Weather Surveillance Radar, 1988 Doppler) radars provides precipitation estimates across the United States [*Klazura and Imy,* 1993]. The precipitation estimates are used operationally by the National Weather Service (NWS) for weather forecasting, flash flood prediction, and as input to hydrologic models for streamflow forecasting. These estimates have potential nonoperational uses as well. The Global Energy and Water Cycle Experiment (GEWEX) Continental-Scale International Project (GCIP) will rely heavily on NEXRAD precipitation estimates for hydrological, meteorological, and climatological studies at a wide range of spatial and temporal scales [*Leese,* 1996]. GCIP activities in the Mississippi River basin require precipitation estimates for diverse landscapes, including the prairie and agricultural areas of the Great Plains and Midwest and the complex mountainous terrain of the Appalachian and the Rocky Mountains along the basin boundary.

[1]Iowa Institute of Hydraulic Research and Department of Civil and Environmental Engineering, University of Iowa, Iowa City.

[2]Department of Civil Engineering and Operations Research, Princeton University, Princeton, New Jersey.

[3]School of Civil and Environmental Engineering, Georgia Institute of Technology, Atlanta.

Paper number 1999JD900123.
0148-0227/99/1999JD900123$09.00

Over the years, extensive development and testing of the WSR-88D and its algorithms have been carried out in the Southern Plains [*Fulton et al.,* 1998]. This is due in part to the potential benefits of WSR-88D technology for enhancing prediction of strong storms and severe weather in this active weather region. The region is also favorable for making radar measurements because of its low topographic relief. In mountainous regions, weather radars need to be sited carefully so that nearby terrain does not block the path of the beam. Site-specific sampling strategies may also be required to avoid beam blockage from distant high mountains, including the use of higher radar beam tilts to see beyond obstacles. The complex terrain that makes radar siting and measurement more difficult also has a profound impact on precipitation patterns. Airflow over topographic barriers enhances storm precipitation [*Houze,* 1993; *Barros and Lettenmaier,* 1994] and produces significant spatial variations in long-term accumulations [*Daly et al.,* 1994]. Topography can also serve to focus storm development during extreme flood-producing rainstorms [*Schwartz,* 1970; *Schroeder,* 1977; *Maddox et al.,* 1978, 1979; *Caracena et al.,* 1979; *Caracena and Fritsch,* 1983; *Maddox and Grice,* 1986; *Hirschboeck,* 1987; *Tucker and Reiter,* 1989; *Smith et al.,* 1996b].

In a recent evaluation of NEXRAD precipitation estimates for the Southern Plains region, *Smith et al.* [1996a] found that systematic biases are present, even in this favorable region for radar measurement. Biases in estimates strongly depend on the distance from the radar. Still, at all distances from the radar, the radar underestimates hourly precipitation accumulations compared to gages. In this paper, we extend

the study of *Smith et al.* [1996a] to evaluate precipitation estimates from the NEXRAD radar in the complex terrain of the northeastern United States. The unique problems associated with precipitation estimation in mountainous terrain are examined on the basis of analyses of two radars in the northern Appalachian Mountains, comparisons with nearby gage estimates, and comparisons with the study results from the Southern Plains. The implications for radar-rainfall estimation in regions of complex terrain are discussed.

2. Study Area and Data Resources

The evaluation of NEXRAD precipitation estimates is made using hourly digital precipitation (HDP) products [*Klazura and Imy,* 1993; *Smith et al.,* 1996a; *Fulton et al.,* 1998] for the Albany (ENX) and Binghamton (BGM) radars in New York state. Figure 1 shows the topography surrounding the two radars. Albany is located in the Hudson River valley and is surrounded by the Adirondack Mountains to the north and the Catskill Mountains to the south. The Albany radar is located in the mountains to the southwest of the city at an elevation of 557 m mean sea level (msl). The Binghamton radar is located in the Appalachian Plateau region at an elevation of 490 m msl. The Catskill Mountains, with peaks as high as 1281 m, are located directly between the two radar sites.

The evaluation of radar precipitation estimates from the two radars is based on hourly digital precipitation (HDP) products collected over a 23-month period (August 5, 1996 through June 30, 1998). The HDP products used in this study are compiled and archived at Princeton University. The raw data product archives

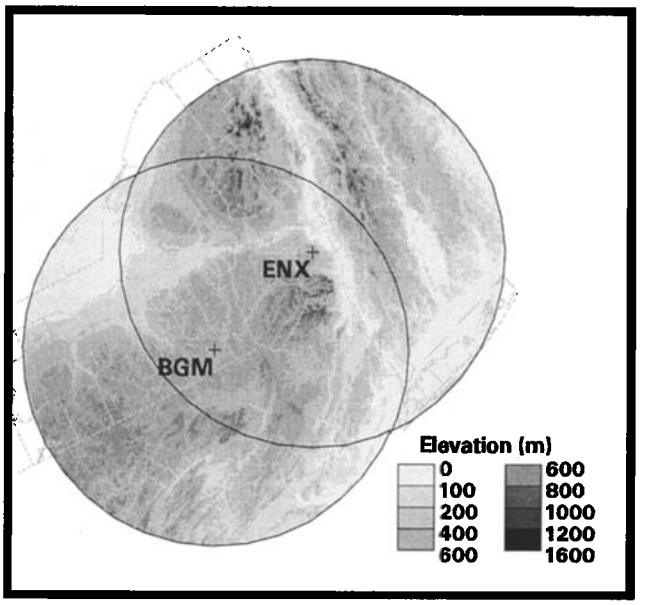

Figure 1. Topography surrounding the Binghamton (BGM) and Albany (ENX) radars.

Table 1. Classification of Radar Data

Classification	Percent of Hours	
	Binghamton	Albany
Accepted	88.8	92.1
Rejected (a)	8.0	5.7
Rejected (b)	3.2	2.2

Radar data are rejected from the analyses if (a) they are flagged as bad during NEXRAD Stage II processing or (b) rejected by a seperate quality control check.

precipitation estimates in 256 logarithmic data levels, ranging from approximately 1 mm/h up to the maximum rain rate imposed by the reflectivity cap. To facilitate data analyses, the HDP products were converted to a compact run-length encoded format [*Kruger and Krajewski,* 1997]. Radar data that were flagged as bad in NEXRAD Stage II processing or were rejected by a separate quality control check were excluded from the analyses in this paper. The quality control criteria eliminated zero or missing radar scans when gage records indicated that there was significant precipitation over the region. Table 1 presents the resulting classification of radar data.

Comparisons are made with hourly precipitation data from gages within the 230 km range of the two radars. These data were obtained from the National Climatic Data Center (NCDC) for the 23-month period. Precipitation accumulations from the available gages have a resolution of either 0.01 or 0.1 inches. Gages with 0.1 inch resolution are more numerous, but their coarse resolution limits their utility for comparisons with radar measurements. For example, until the accumulation reaches 0.1 inches, the gage reports zero accumulation. As a result, estimates of hourly precipitation statistics are affected by the gage resolution.

3. NEXRAD Precipitation-Processing Algorithms

A brief description of the WSR-88D radar and the NEXRAD precipitation-processing algorithms is given in this section. For detailed information on methods used for precipitation estimation using WSR-88D data, see *Fulton et al.* [1998], *Klazura and Imy* [1993], *Smith et al.* [1996a], and *Baeck and Smith* [1998].

The NEXRAD precipitation algorithms utilize a power law Z-R relationship:

$$R = aZ^b \tag{1}$$

where R is rainfall rate (mm/h), a and b are adjustable parameters, and Z is the radar reflectivity factor (mm^6/m^3). The radar reflectivity factor Z is estimated from the radar-measured backscatter power, which de-

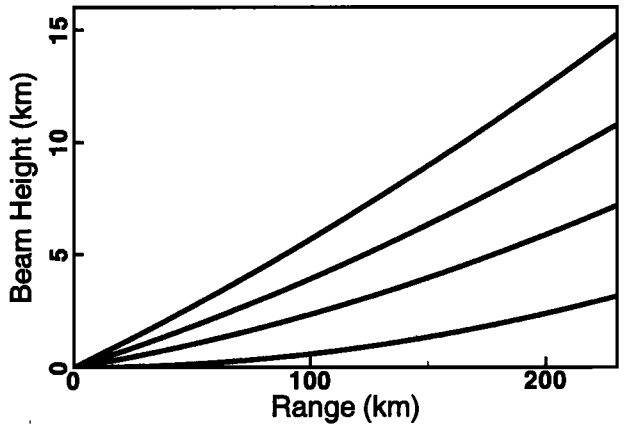

Figure 2. Mean beam heights for the four tilts used for NEXRAD precipitation estimation (0.5, 1.5, 2.4, and 3.4 degrees).

pends (in part) on the number and size of hydrometeors in the sampling volume. The default Z-R parameters for the NEXRAD algorithms are $a = 0.017$ and $b = 0.714$ (conventionally expressed in the form $Z = 300R^{1.4}$). A tropical Z-R relationship ($Z = 250R^{1.2}$) is used on occasion for events dominated by warm rain microphysics [*Smith et al.*, 1996b].

Several aspects of radar measurement of reflectivity are crucial for assessing radar-rainfall estimates in complex terrain. The radar samples a volume of the atmosphere, the size of which increases with distance from the radar. For the WSR-88D rainfall algorithms, radar reflectivity values are utilized in a polar coordinate system with resolution of approximately 1° in azimuth by 1 km in range. Multiple 360° sweeps are obtained at beam angles ranging from 0.5° to 20° from the horizon. Figure 2 shows the mean beam elevation versus range for the four lowest radar tilts. The field of radar reflectivity factor values used in estimating rainfall is derived from these tilts of the radar beam, with higher tilts being used closer to the radar and the low tilts at far range. The paired objectives of this hybrid-scan sampling strategy [see *Fulton et al.*, 1998] are (1) to sample rainfall as close to the ground as possible and (2) to minimize contamination of rainfall estimates by ground returns. In complex terrain these objectives are especially challenging to achieve simultaneously. In addition, the hybrid-scan strategy must be constructed to avoid ground returns and serious beam blockage from high-elevation regions. Consequently, the tilt selection will not necessarily vary in regular fashion with range from the radar. The hybrid scan strategies for the Albany and Binghamton radars are depicted in Figure 3. These scan strategies have recently been replaced with new, terrain-based versions, which should improve precipitation estimation within 50 km of the radar [*O'Bannon*, 1997].

Several additional elements of the WSR-88D rainfall algorithms are particularly relevant for mountainous regions. Beams that are partially blocked can be used at a farther range through the application of an occultation correction, which adds power to the radar measurement based on the fraction of power that is lost at closer range through blockage. Occultation corrections can be several decibels in magnitude. *Creutin et al.* [1997] evaluate a similar scheme for correction of par-

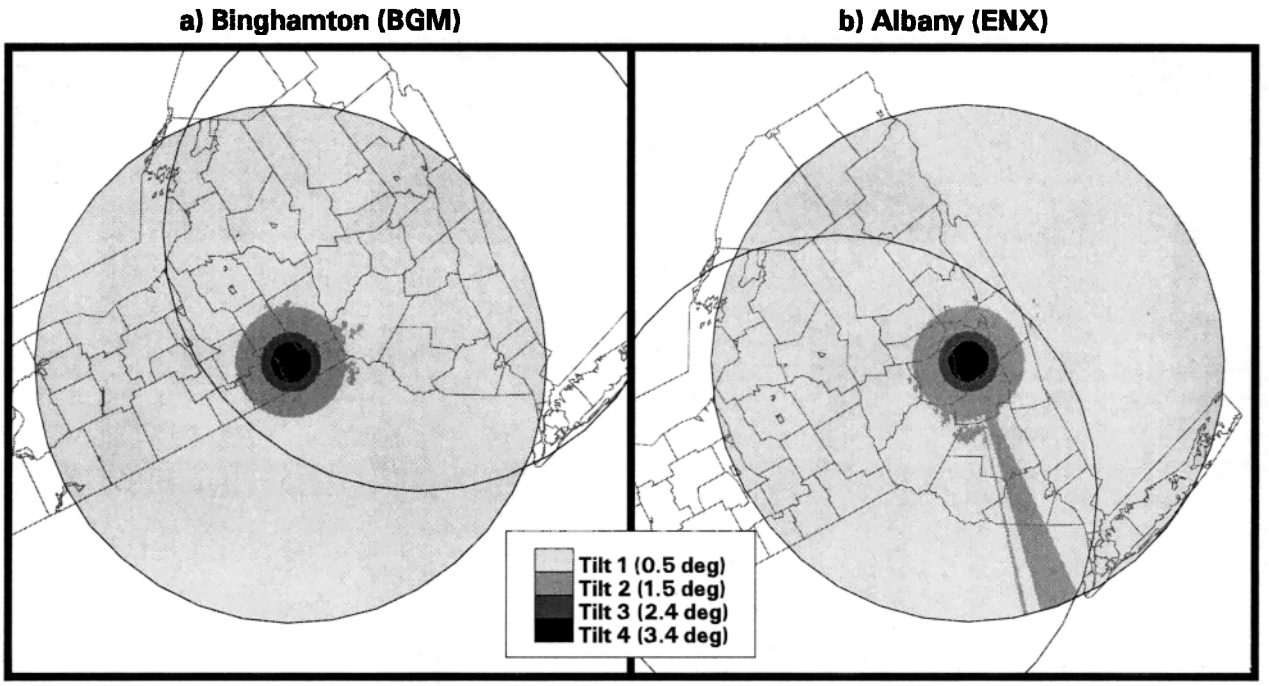

Figure 3. Hybrid scanning strategy for the (a) Binghamton (BGM) and (b) Albany (ENX) radars.

tial blockage. The algorithms used for detecting and elimination of ground returns are of special relevance to complex terrain. Doppler velocity measurements from clear air mode are used periodically to construct ground clutter maps, and reflectivity thresholds are used for removing high returns from isolated targets. The tilt-test algorithm computes the percent reduction in echo area from the first tilt to the second tilt. If the echo area reduction exceeds a specified magnitude, the low tilt is presumed to be contaminated by anomalous propagation (AP) returns and the second tilt is used in its place [*Fulton, et al.*, 1998].

The rain rate estimates from the WSR-88D are used by the NWS in the NEXRAD Precipitation Processing System (PPS). First, rain rate intensity maps are integrated over time to produce hourly rainfall accumulations. Results are then converted from the polar coordinates of the radar to a Hydrologic Rainfall Analysis Project (HRAP) grid of approximately 4 × 4 km. The HRAP grid is a polar stereographic projection that conforms to a 1/40th limited fined mesh (LFM) grid used by the NWS in numerical weather prediction [*Reed and Maidment*, 1998].

4. Radar Precipitation Evaluation

This section evaluates HDP estimates for the Binghamton and Albany radars based on observed probability of precipitation, conditional mean precipitation, and mean hourly accumulation. The probability of precipitation is defined as the fraction of hours recording precipitation. The conditional mean hourly precipitation is the average accumulation for hours with precipitation. The mean hourly accumulation is the total observed precipitation divided by the number of hours on record. Both the range dependence and the spatial distribution of these quantities are evaluated.

4.1. Range-Dependent Variations

Range-dependent biases are present in NEXRAD precipitation estimates due to the effects of range on the size and height of the radar-sampling volume [*Smith et al.*, 1996a]. Figure 4 shows range-dependent variations in probability of precipitation, conditional mean hourly precipitation, and mean hourly accumulation for the two radars for the warm (April-September) and cold (October-March) seasons. The warm season probability of precipitation increases slightly from the radar to the 50 km range. However, the Albany radar exhibits an isolated peak in probability at 60 km, while the Binghamton radar remains fairly constant from 50 to 150 km. For both radars, probability of precipitation declines sharply from 150 to 230 km. In the cold season the peak in precipitation probability for the Albany radar is more pronounced than for the warm season but is still located at 60 km from the radar. The cold season decline in probability begins closer to the radar, and the decrease is dramatic. The probability of precipitation is almost zero at 230 km. This decline in probability with range is due to partial blockage of the beam and beam overshoot. Partial blockage may reduce echoes to below NEXRAD detection thresholds. At long ranges the beam height is several kilometers above the ground (see Figure 2). Precipitating clouds often form below this level and thus avoid radar detection. This effect is especially pronounced during the cold season, when a significant portion of precipitation results from low stratiform clouds.

The two radars show opposite trends in the conditional mean precipitation during the warm season. The Binghamton radar is at a minimum near the radar and exhibits a maximum near 230 km. The Albany conditional mean decreases slightly with range. However, for the cold season, the two radars exhibit a similar trend in conditional mean precipitation. Both show a gradual decrease from near the radar to 230 km, with a dip at 60 km. The mild range dependence of conditional mean precipitation suggests that a range correction algorithm would not significantly improve precipitation estimates as long as detection problems persist.

The mean precipitation is a combination of the probability of precipitation and the conditional mean. In the warm season the Albany mean precipitation peaks at 60 km due to the peak in probability of precipitation. It then decreases with range, especially after 160 km, due in large part to the decrease in probability of precipitation. The Binghamton mean precipitation has a local peak at 40 km and increases gradually to 160 km due to the increases in conditional mean with range. The mean precipitation decreases at longer ranges, as the effect of lower probabilities of precipitation overwhelms the increases in conditional mean. During the cold season, the probability of precipitation dominates the mean accumulation for both radars. Interestingly, the peak in probability at 60 km for the Albany radar is canceled by the dip in conditional mean. The mean precipitation for both radars increases from the radar to 20 km. The Albany mean remains fairly steady to 100 km and then decreases sharply to 230 km, while the Binghamton mean plunges from 40 to 50 km, remains steady to 125 km, and then drops with the Albany mean.

There are some noteworthy differences in the range dependent characteristics of the radar precipitation for the study area and the Southern Plains region [*Smith et al.*, 1996a]. First, precipitation detection is a more significant problem in the northern Appalachians. Although a decrease in the probability of precipitation with range was also observed in the Southern Plains, the decrease there was much less pronounced. In the northern Appalachians, detection problems in the cold season are so severe that the effective range of the WSR-88D radar is reduced. Second, the strong variations in the conditional mean, which were observed in the Southern Plains, are not observed in the northern Ap-

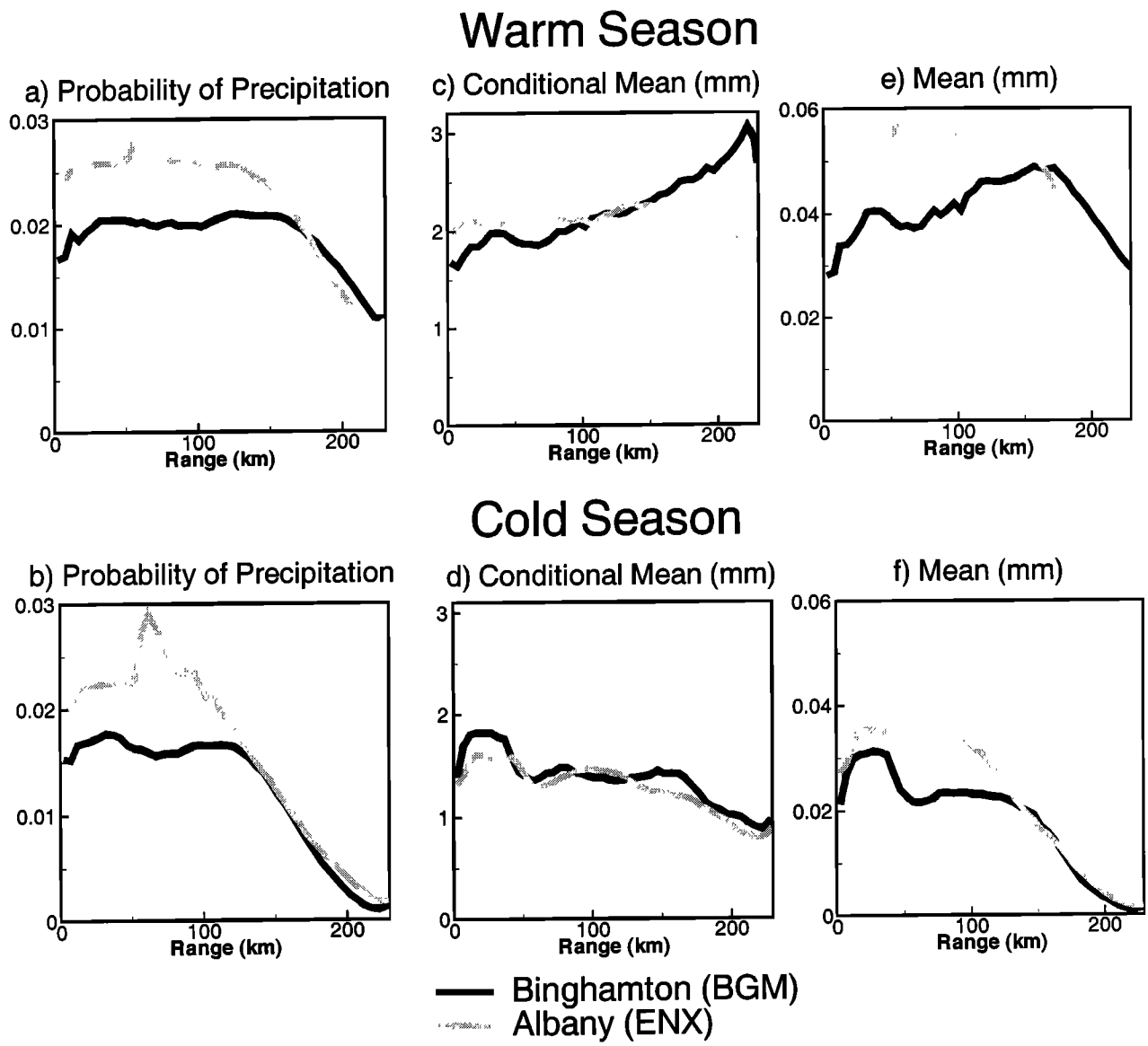

Figure 4. Radar characteristics versus range (km) from the radar site for the Binghamton (BGM) and Albany (ENX) radars for the warm season (April-September) and cold season (October-March).

palachians. *Smith et al.* [1996a] note that the variations are a result of two factors. The biscan maximization scheme for constructing the hybrid scan from multiple radar tilts creates (negative) biases near the radar, and bright band echoes, which result from melting precipitation, produce (positive) biases at slightly longer ranges. In recent years the biscan maximization scheme has been eliminated from the algorithm, and it was not in use for the Albany and Binghamton radars. *Baeck and Smith* [1998] show that this improvement has significantly reduced the range-dependent variations in conditional mean precipitation.

4.2. Spatial Variations

The complex topography of the study region produces spatially biased radar precipitation estimates. Figure 5 shows the probability of precipitation based on the Binghamton and Albany radars for the 23-month period. The circular features for the two radars clearly show the effects of range on precipitation detection. Still, other features are evident. For the Binghamton radar, there is acute beam blockage south of the radar. For the Albany radar, there is widespread beam blockage to the southwest of the radar. The Catskill Mountains obstruct radar visibility, forcing use of higher beam tilts (see Figure 3). The Albany radar also records very high probability of precipitation in nearby areas of elevated topography, as shown in Figure 6. This is likely due to ground returns from the mountains rather than enhanced orographic precipitation. The location of the high probability areas, which are confined to the north and east of the radar, suggests that the path of the

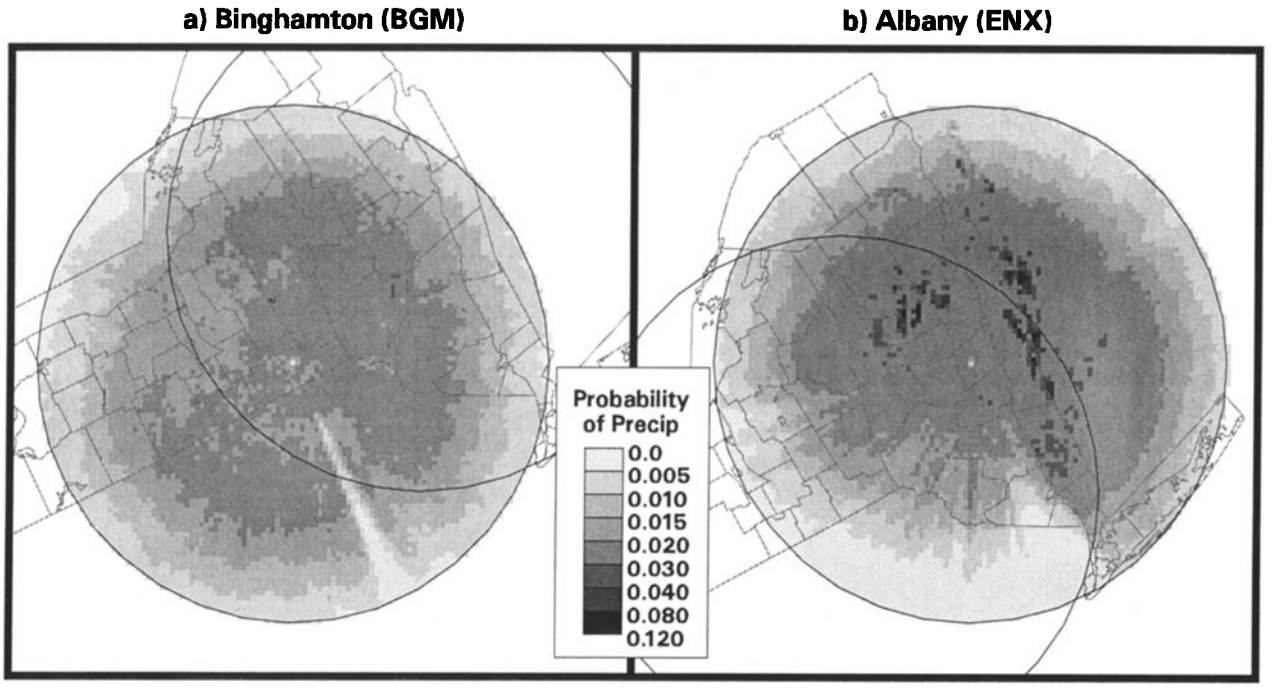

Figure 5. Probability of precipitation for the (a) Binghamton (BGM) and (b) Albany (ENX) radars.

radar beam may be affected by the local atmospheric conditions over the Mohawk and Hudson Rivers. Note that the locations of high probabilities are from 50 to 100 km from the radar, which explains the isolated peak in precipitation probabilities at the 60 km range.

Figure 7 shows the conditional mean hourly precipitation for the two radars for the 23-month period. For the Binghamton radar, high conditional means at the fringes are evident. Very high conditional means are seen near the fringe in the beam blockage area to the south of the radar. The high condition means at the fringe and in the beam blockage area are a result of two factors. First, precipitation detection is low at these ranges, which greatly reduces the number of observations available for computation of the mean. Second, the occultation correction to account for partial beam blockage adds power to the radar measurements, which results in higher precipitation estimates. These two factors explain the increase in conditional mean observed in the warm season for the Binghamton radar in Figure 4.

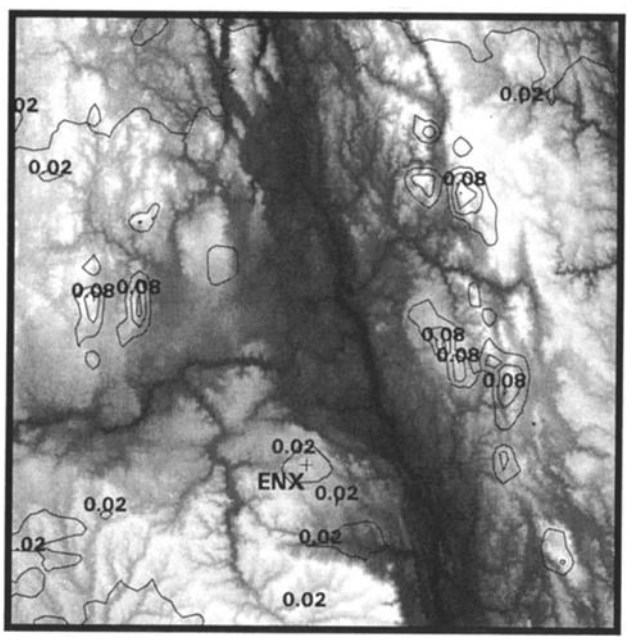

Figure 6. Contoured probability of precipitation for the Albany (ENX) radar overlayed on topography.

For the Albany radar, beam blockage also has a clear effect on spatial patterns of conditional mean precipitation. The highest conditional means are concentrated to the south of the radar, in the region blocked by the Catskill Mountains. Again, these are a result of the effects of limited and selective detection of precipitation in blocked areas and the occultation correction. In contrast, the highest probabilities of precipitation near the Albany radar are associated with slightly lower conditional mean precipitation than their surrounding areas. This indicates that the ground returns responsible for the high probabilities are persistent but weak.

For both radars, very high conditional means are present for isolated areas in high mountain regions. These are seen in Figure 7 to the northeast and southwest of the Binghamton radar and to the north of the Albany radar. Although higher precipitation rates for elevated terrain are possible, it is likely that these higher conditional means are associated with ground returns. Bending of the radar beam under certain atmospheric conditions may be sufficient to cause the beam to inter-

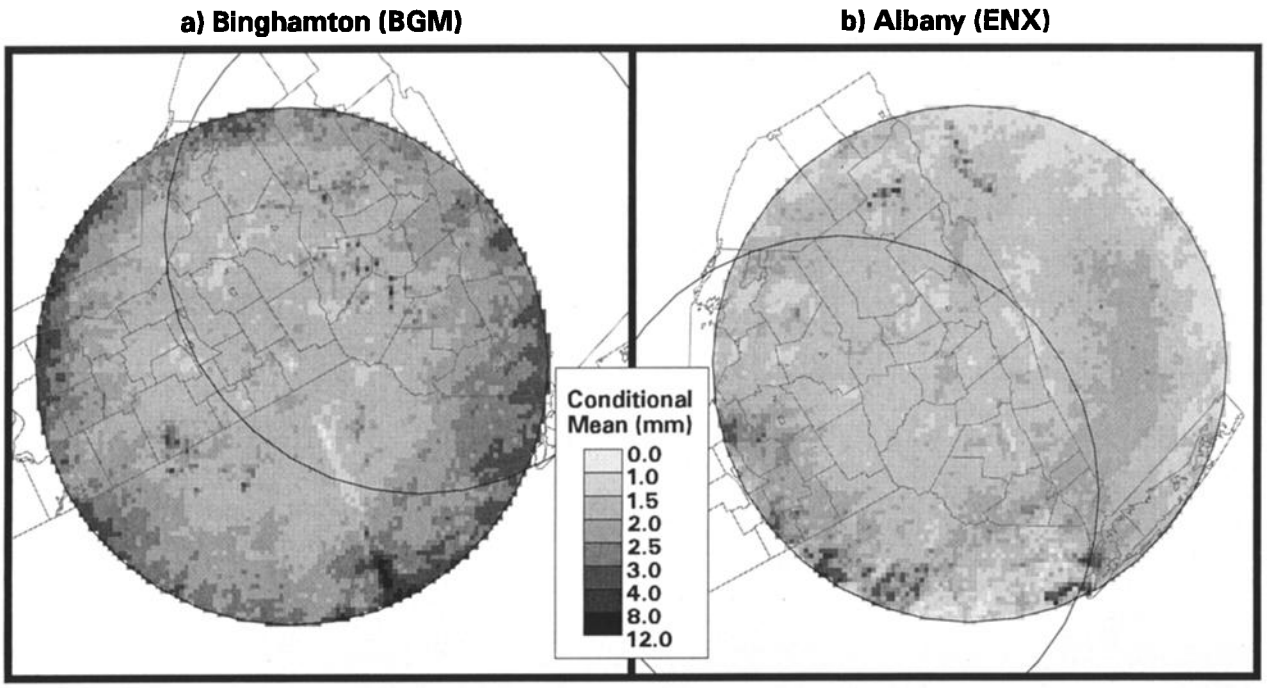

Figure 7. Conditional mean hourly precipitation (mm) for the (a) Binghamton (BGM) and (b) Albany (ENX) radars.

sect high terrain but not elsewhere. Analysis of hourly and storm total accumulations shows that these returns range over multiple adjacent radar cells and are imbedded in precipitation. Thus the resulting echoes would not be classified as AP returns using the NEXRAD tilt-test algorithm and are too widespread to be classified as isolated targets. To correct for this problem, improved algorithms, which are aware of the surrounding terrain, may be needed for identification of such ground returns.

5. Radar-Radar Biases

Analysis of the overlap region for the Binghamton and Albany radars demonstrates the complexity of radar-rainfall estimation in mountainous regions. Figure 8 compares coincident radar measurements for the warm and cold seasons. Table 2 presents summary statistics for these six graphs. Comparisons include estimates of fractional coverage of precipitation, conditional mean hourly precipitation, and mean hourly accumulation for the overlap region. In this section the fractional coverage is defined as the fraction of overlap cells, in 1 hour, which observe precipitation; the conditional mean is the spatial average for all overlap cells recording nonzero precipitation; and mean precipitation is computed for the entire overlap region.

Good agreement in fractional coverage supports the belief that delineation of the precipitating area is a particular strength of weather radar [*Smith et al.*, 1996a; *Moore and Smith,* 1972]. However, Figure 8 shows that differences in fractional coverage for the two radars are significant. The correlation coefficient for fractional coverage is 0.92 for the warm season and 0.82 for the cold season. *Smith et al.* [1996a] found that radar intercomparisons for the Southern Plains region show very good agreement in fractional coverage. This study suggests that delineation of the precipitating area is less accurate in mountainous regions.

The conditional mean and mean precipitation compare quantitative precipitation estimates for the two radars in the overlap region. Figure 8 shows that there are large differences in coincident precipitation estimates. The scatter in the relations are greater in the cold season, although the root-mean-square difference (RMSD) is high (1.12 mm) for the warm season conditional mean. There are also several hours when precipitation is detected over the area for one radar but not for the other. Although some cases could be mistakes in the archived records (i.e., records indicate that the radar was operating and data are available), many are probably associated with hours where precipitation was undetected in the overlap region by one of the radars or falsely detected by the other.

Spatial variations in radar biases contribute to the uncertainty in radar intercomparisons for the overlap region. Figure 9 shows the difference between the probability of precipitation for the Binghamton (BGM) and Albany (ENX) radars for the 23-month period. In the overlap region, probabilities for the Binghamton radar are higher in the half nearer the radar and vice versa for the Albany radar. Large positive differences in the south are due primarily to blockage of the Albany radar

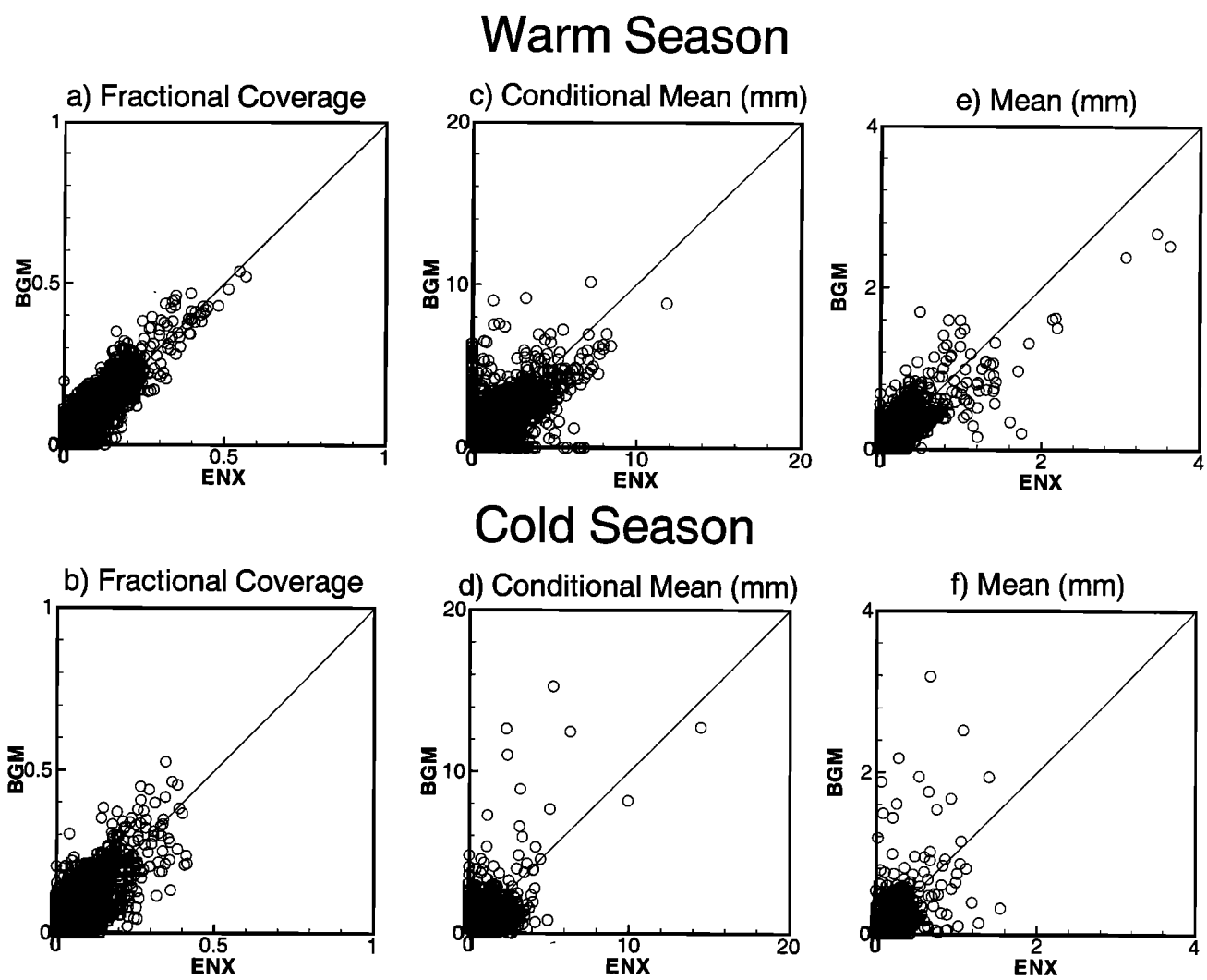

Figure 8. Comparison of radar characteristics for overlap areas of the Binghamton (BGM) and Albany (ENX) radars for the warm season (April-September) and cold season (October-March).

by the Catskill Mountains. Figure 10 shows the difference between the mean precipitation conditioned on both radars detecting precipitation. Again, the biases shown are strongly linked to range effects. The high positive biases in the southern portion of the overlap region result from detection problems. The Albany radar uses a higher tilt for part of this region and thus detects only the top of deep, convective clouds. Because the Binghamton radar samples these clouds closer to the ground, the discrepancy in precipitation estimates is high. Also note that the sample size for this analysis is quite low (of the order of 30 hours for the entire study period), because the Albany radar rarely detects precipitation for this region.

Table 2. Comparison of Radar Estimates for the Overlap Region, Including the Correlation and Root-Mean-Square Difference for the Fractional Coverage and the Conditional and Unconditional Spatial Averages

	Warm Season	Cold Season
Fractional coverage		
correlation	0.92	0.82
RMSD, %	0.03	0.04
Conditional mean		
correlation	0.61	0.58
RMSD, mm	1.12	0.81
Mean precipitation		
correlation	0.85	0.61
RMSD, mm	0.12	0.16

The results of this intercomparison indicate that there are significant differences in radar observations in mountainous terrain. Range-dependent and terrain-dependent biases limit the ability of a single radar to observe precipitation occurrence and estimate precipitation accumulations over the entire radar umbrella. Methods for merging precipitation estimates from multiple radar will be critical for accurate estimation of precipitation in these regions. Still, further research on optimal approaches for merging estimates from multiple radars in complex terrain is needed.

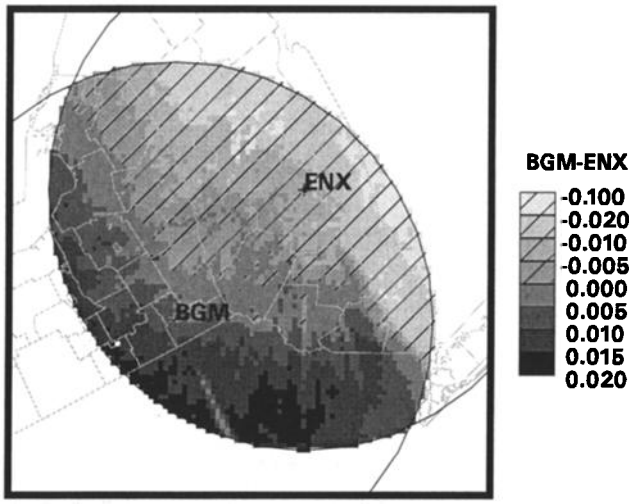

Figure 9. Difference between the probability of precipitation for the Binghamton (BGM) and Albany (ENX) radars for period from August 1996 through June 1998.

6. Radar-Gage Comparison

A comparison of radar-rainfall estimates and gage observations is made for the 23-month period to evaluate biases in precipitation accumulation and detection. The comparisons presented in this section are based on 97 gages within the 230 km umbrella of the Binghamton radar and 93 gages within range of the Albany radar. Because the results of the radar-gage comparison are similar for both radars, results are presented for the Binghamton radar only.

In such a comparison it is important to recognize the differences in spatial sampling of precipitation for the two sensors [*Austin,* 1987; *Ciach,* 1997]. A typical 8-inch rain gage samples precipitation over an area of 0.3 m^2, while radar samples precipitation within a volume and estimates the average accumulation over an area (in this case approximately 4×4 km). As a result, there are inherent differences in precipitation estimates from these two sensors [*Ciach and Krajewski,* 1998].

Figure 11 compares Binghamton radar hourly accumulations with gage observations for two ranges for the warm and cold seasons. Hourly accumulations are shown for periods when the gage or the radar records nonzero precipitation. Several features are worth noting. First, at the hourly time step the differences in gage resolution are apparent. For gages with 0.1 inch resolution, accumulations are grouped into a few discrete values, making a comparison more difficult. Still, based on these measurements and those for gages with 0.01 inch resolution, it is clear that variability between radar and gage estimates at the hourly time step is high. For the warm season, the RMSD is 4.5 mm for ranges of 160 km or less and 5.7 mm for ranges greater than 160 km. For the cold season, the RMSD is 3.3 mm for ranges of 160 km or less, and 3.3 mm for ranges greater than 160 km. In addition, the radar precipitation estimates tend to be lower than the gage estimates, especially in the cold season and at longer ranges from the radar. These results are similar to those for the Southern Plains. *Smith et al.* [1996a] also observed significant scatter in radar-gage comparisons and a systematic underestimation of precipitation by the radar. However, the scatter is much greater in the northern Appalachians, and the seasonal differences are more pronounced.

On an hourly timescale, spatial variations in precipitation and the effects of gage resolution significantly contribute to the mismatch in radar and gage estimates. However, integrating over longer timescales minimizes these factors, revealing systematic biases in the radar estimates. Figure 12 shows the total accumulation for the Binghamton radar and gages for the warm and cold season. The underestimation of the radar is significant in both seasons but is more pronounced in the cold season. For the warm season, the average radar precipitation is 39.8% of the gage estimate. For the cold season, the average radar precipitation is 9.3% of the gage estimate.

The radar evaluations in section 4 show that precipitation detection suffers at long ranges due to the range dependence of radar sampling. A comparison of radar and gage detection of precipitation is made in Figure 13, which shows the probability of precipitation at one sensor (i.e., the radar or the gage) conditioned on detection of precipitation at the other sensor. When precipitation is detected by the radar, the probability that precipitation is detected by the gage is high. The average detection for 0.01 inch resolution gages is 67.6% in the warm season and 80.5% in the cold season. For 0.1 inch resolution gages the percentages are lower. This is not unexpected, since larger accumulations are required before these gages will indicate nonzero precipitation.

Given the mismatch in the measurement area of the two sensors, it is difficult to draw conclusions regarding

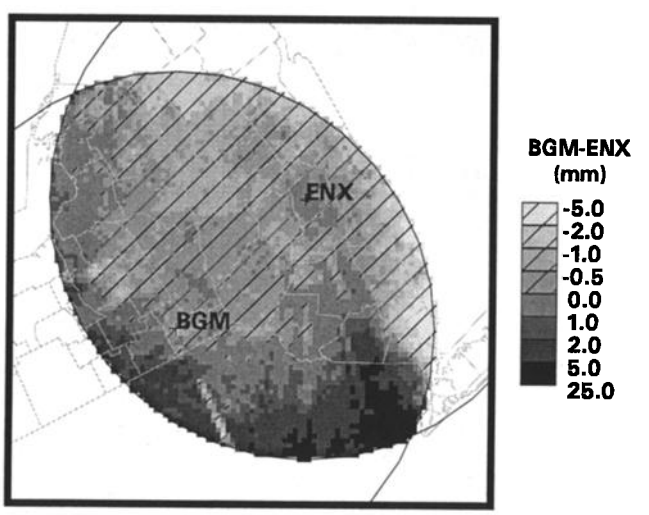

Figure 10. Difference between the conditional mean precipitation for the Binghamton (BGM) and Albany (ENX) radars for the period August 1996 through June 1998. Note that the mean precipitation is conditioned on both radars recording non-zero precipitation.

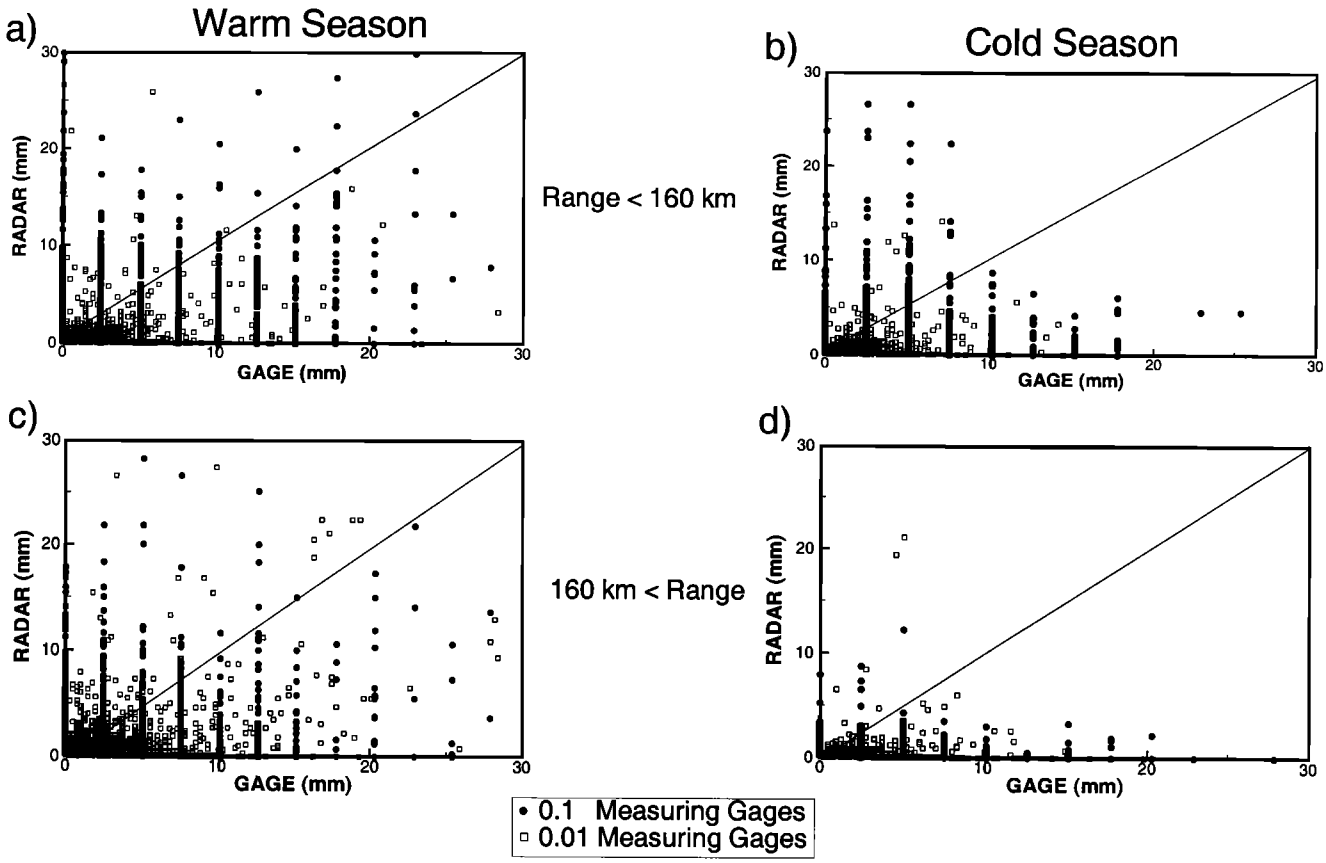

Figure 11. Comparison of radar and gage hourly precipitation accumulation (mm) for the Binghamton (BGM) radar for the warm season (April-September) and cold season (October-March).

radar quality from Figure 13a. However, when precipitation is detected by the gage, one expects very high probabilities of detection for the radar. Figure 13b shows that the probability that precipitation is detected by the radar is surprisingly low. For all gages the average radar detection is 31.0% in the warm season and 14.4% in the cold season. Although the low precipitation detection by radar is common at all ranges, the problem is most severe during the cold season and at longer ranges. Table 3 shows the average probability that precipitation is detected by the radar given that the measured gage precipitation exceeds various thresholds ranging from 0 to 1.0 inches for all the gages within the range of the Binghamton radar. As expected, for higher gage precipitation thresholds the probability of detection by the radar increases. Still, the probability of detection by the radar remains low, especially in the cold season. These results indicate a serious prob-

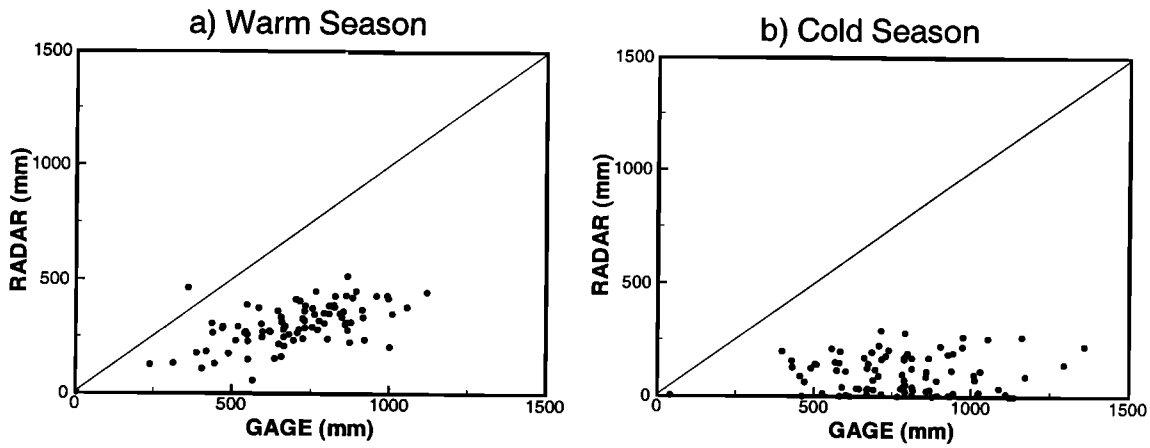

Figure 12. Comparison of radar and gage total precipitation accumulation (mm) for the Binghamton (BGM) radar for the warm season (April-September) and cold season (October-March).

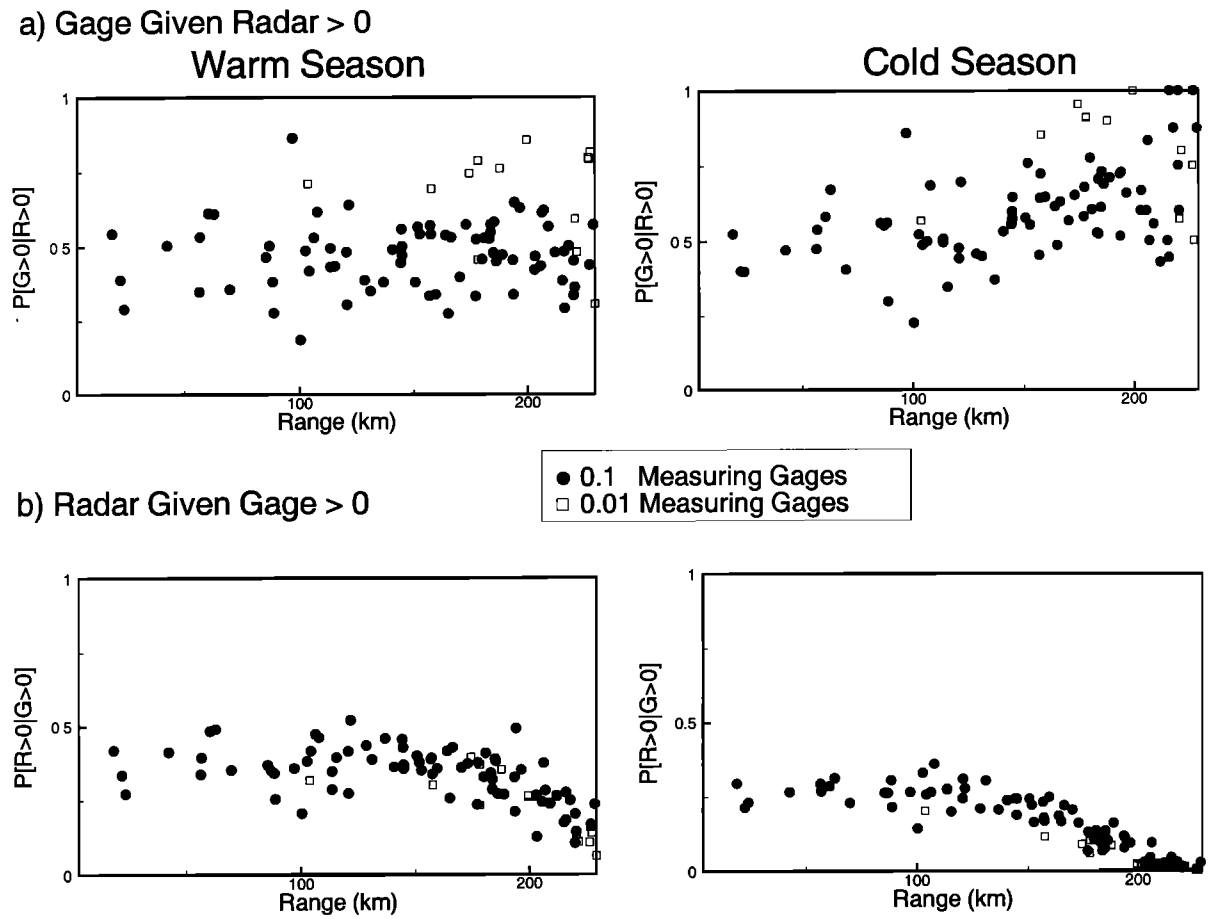

Figure 13. Probability of precipitation for the Binghamton (BGM) radar for a) Gage given Radar > 0 for warm season (April-September) and cold season (October-March), and b) Radar given Gage > 0 for warm season (April-September) and cold season (October-March).

lem with radar precipitation detection in mountainous areas. In contrast, precipitation detection in the Southern Plains by radar and gage is very consistent [*Smith et al.*, 1996a].

The radar-gage comparison suggests that two factors contribute to the significant underestimation of long-term precipitation accumulations. First, there is a systematic underestimation of hourly accumulation when precipitation is detected by the radar, as shown in Figure 11. This underestimation was also observed in the Southern Plains. A second factor is failure of the radar to detect precipitation. This problem is unique to the complex mountainous terrain. Although improvements in precipitation algorithms could reduce the estimation biases, detection problems will remain an issue because they are linked to both the unique precipitation processes and the difficulties associated with precipitation measurement in mountainous areas.

Table 3. Probability of Precipitation Detection by the Radar (R) Given That the Gage (G) Detects Precipitation Greater Than a Threshold x

	Warm Season		Cold Season	
x(inch)	N	$P[R > 0 \mid G > x]$	N	$P[R > 0 \mid G > x]$
0.0	18946	0.3098	26652	0.1436
0.1	4754	0.5644	4097	0.3285
0.5	526	0.7890	121	0.7190
0.75	113	0.8673	7	1.0000
1.0	47	0.9362	1	1.0000

N indicates the number of times the gages detect precipitation greater than the threshold x.

7. Summary and Conclusions

The complex terrain of the northern Appalachians complicates radar-based estimation of precipitation. Beam blockage, ground returns, and nondetection and underestimation of precipitation are all problematic for the two radars evaluated in this study.

Beam blockage, and the consequent use of higher tilts, causes significant detection problems at long ranges. Cold season detection is more problematic than warm season detection. The nondetection of precipitation is much worse than reported for the Southern Plains and suggests that the effective range of WSR-88D radars is reduced in mountainous regions. Furthermore, the occultation correction employed to account for partial beam blockage has serious limitations. The conditional mean hourly accumulation for the Binghamton radar in the warm season actually increases with range. This effect is exaggerated along the beam blockage to the south.

The spatial distributions of conditional mean and probability of precipitation indicate that ground returns from anomalous propagation and ground clutter cause unique precipitation estimation biases in mountainous regions. Variations in elevation across the study region make detection of ground returns difficult, because high reflectivity values may occur only in areas with high mountains.

Radar-gage comparisons demonstrate that nondetection and underestimation are severe for the two radars. Even when both the gage and the radar record precipitation at the same time, the radar consistently underestimates precipitation. Detection and underestimation are problems for both the warm and the cold seasons but are most severe for the cold season and at long ranges.

Improved algorithms are needed for radar-based precipitation estimation in complex mountainous terrain. These new algorithms must account for systematic biases due to range dependence, beam blockage, and complex terrain. Although improved calibration of the radar-rainfall algorithm [*Anagnostou and Krajewski,* 1998] or conversion to a multiparameter polarimetric radar may reduce bias in estimation, the problem of nondetection must still be addressed in mountainous regions. Possible solutions include the use of multiple radars to develop reflectivity and precipitation maps.

Acknowledgments. This study was funded in part by the New York City Department of Environmental Protection (NYDEP), by an NSF Graduate Fellowship, and NSF grant CMS-9702715. This support is gratefully acknowledged. Special thanks go to Wolfe Tone and Dominique Thongs at NYDEP for their help throughout the project. Special thanks are also due to Timothy O'Bannon of the NEXRAD Operational Support Facility and Dong-Jun Seo of the Hydrologic Research Laboratory for supplying the hybrid-scan strategies. The authors sincerely appreciate the thorough comments of an anonymous reviewer.

References

Anagnostou, E. N., and W. F. Krajewski, Calibration of the WSR-88D precipitation processing subsystem, *Weather Forecasting, 13*(2) 396–406, 1998.

Austin, P., Relation between measured radar reflecivity and surface rainfall, *Mon. Weather Rev., 115*, 1053–1070, 1987.

Baeck, M. L., and J. A. Smith, Rainfall estimation by the WSR-88D for heavy rainfall events, *Weather Forecasting, 13*(2), 416–436, 1998.

Barros, A. P., and D. P. Lettenmaier, Dynamic modeling of orographically induced precipitation, *Rev. Geophys., 32*(3), 265–284, 1994.

Caracena, F., and J. M. Fritsch, Focusing mechanisms in the Texas Hill Country flash floods of 1978, *Mon. Weather Rev., 111*, 2319–2332, 1983.

Caracena, F., R. A. Maddox, L. R. Hoxit, and C. F. Chappell, Meso-analysis of the Big Thompson storm, *Mon. Weather Rev., 107*(1), 1–17, 1979.

Ciach, G. J., Radar rainfall estimation as an optimal prediction problem, 230 pp., Ph.D. dissertation, Dep. of Civ. and Environ. Eng., Univ. of Iowa, Iowa City, 1997.

Ciach, G. J., and W. F. Krajewski, On the estimation of radar rainfall error variance, *Advances in Water Resources, 22*(6), 1999.

Creutin, J. D., H. Andrieu, and D. Faure, Use of a weather radar for the hydrology of a mountainous area, II, Radar measurment validation, *J. of Hydrol., 193*, 26–44, 1997.

Daly, C., R.P. Neilson, and D.L. Phillips, A statistical-topographic model for mapping climatological precipitation over mountainous terrain, *J. Appl. Meteorol., 33*(2), 140–158, 1994.

Fulton, R. A., J. P. Breidenbach, D.-J. Seo, and D. A. Miller, The WSR-88D rainfall algorithm, *Weather Forecasting, 13*(2), 377–395, 1998.

Hirschboeck, K. K., Catastrophic flooding and atmospheric circulation anomalies, in *Catastrophic Flooding,* edited by L. Mayer and D. Nash, pp. 23-56, Allen and Unwin, Winchester, Mass., 1987.

Houze, R. A., *Cloud Dynamics,* 573 pp., Academic, San Diego, Calif., 1993.

Klazura, G. E., and D. A. Imy, A description of the initial set of analysis products available from NEXRAD WSR-88D system, *Bull. Am. Meteorol. Soc., 74*(7), 1293–1311, 1993.

Kruger, A., and W.F. Krajewski, Efficient storage of weather radar data, *Software Pract. Exp., 27*(6), 623–635, 1997.

Leese, J. A., Major activities plan for 1997, 1998, and outlook for 1999 for the GEWEX Continental-Scale International Project (GCIP), 1, Research, *IGPO Publ. Ser. 25*, Silver Spring, Md., 1996.

Maddox, R. A., and G. K. Grice, The Austin, Texas, flash flood: An examination from two perspectives — Forecasting and research, *Weather Forecasting, 1*, 66–76, 1986.

Maddox, R. A., L. R. Hoxit, C. F. Chappell, and F. Caracena, Comparison of meteorological aspects of the Big Thompson and Rapid City flash floods, *Mon. Weather Rev., 106*, 375–389, 1978.

Maddox, R. A., C. Chappell, and L. Hoxit, Synoptic and meso-α scale aspects of flash flood events, *Bull. Am. Meteorol. Soc., 60*(2), 115–123, 1979.

Moore, P. L., and D. L. Smith, Updating of numerical precipitation guidance, *J. Appl. Meteorol., 11*, 1293–1298, 1972.

O'Bannon, T., Using a 'terrain-based' hybrid scan to improve WSR-88D precipitation estimates, Preprints, in *Proceedings of the 28th Conference on Radar Meteorology,* pp. 506–507, Am. Meteorol. Soc., Boston, Mass., 1998.

Reed, S. M., and D. R. Maidment, Coordinate transformations for using NEXRAD data in GIS-based hydrologic modeling, *J. Hydrol. Eng.*, in press, 1998.

Schwartz, F. K., The unprecedented rains associated with the remnants of Hurricane Camille, *Mon. Weather Rev., 98*(11), 851–859, 1970.

Schroeder, T. A., Meteorological analysis of an Oahu flood, *Mon. Weather Rev., 105*, 458–468, 1977.

Smith, J. A., D. J. Seo, M. L. Baeck, and M. D. Hudlow, An intercomparison study of NEXRAD precipitation estimates, *Water Resour. Res., 32*(7), 2035–2045, 1996a.

Smith, J. A., M. L. Baeck, M. Steiner, and A. J. Miller, Catastrophic rainfall from an upslope thunderstorm in the central Appalachians: The Rapidan storm of June 27, 1995, *Water Resour. Res., 32*(10), 3099–3113, 1996b.

Tucker, D. F., and E. R. Reiter, Heavy rainfall in complex terrain: Insights from a numerical model, *Meteorol. Atmos. Phys., 40*, 194–210, 1989.

M. L. Baeck, Department of Civil Engineering and Operations Research, Princeton University, Princeton, NJ 08544. (e-mail: mlbaeck@radap.princeton.edu)

A. A. Bradley, B. R. Nelson, and C. B. Young, Iowa Institute of Hydraulic Research and Department of Civil and Environmental Engineering, University of Iowa, Iowa City, IA 52252. (e-mail: allen-bradley@uiowa.edu; bnelson@iihr.uiowa.edu; cbyoung@cgrer.uiowa.edu)

A. Kruger, Iowa Institute of Hydraulic Research and Department of Civil and Environmental Engineering, University of Iowa, Iowa City, IA 52252. (e-mail: kruger@iihr.uiowa.edu)

C. D. Peters-Lidard, School of Civil and Environmental Engineering, Georgia Institute of Technology, Atlanta, GA 30332. (e-mail: cpeters@ce.gatech.edu)

J. A. Smith, Department of Civil Engineering and Operations Research, Princeton University, Princeton, NJ 08544. (e-mail: jsmith@radap.princeton.edu)

(Received September 1, 1998; revised December 21, 1998; accepted February 4, 1999.)